Bull. Mater. Sci., Vol. 34, No. 6, October 2011, pp. 1173–1177. © Indian Academy of Sciences.

Synthesis and characterization of polythiophene-modified TiO_2 nanotube arrays

YUWEI LAN[a,b], LIYA ZHOU[a,b], ZHANGFA TONG[a], QI PANG[c,*], FAN WANG[a] and FUZHONG GONG[a]

[a]College of Chemistry and Chemical Engineering of Guangxi University, Nanning 530004, China
[b]Key Laboratory of Semiconductor Materials Science, Institute of Semiconductors, Chinese Academy of Sciences, P.O. Box 912, Beijing 100083, China
[c]College of Chemistry and Material, Yulin Normal University, Yulin, Guangxi 537000, China

MS received 5 March 2011; revised 13 April 2011

Abstract. **The highly ordered and uniform TiO_2 nanotube arrays were fabricated by anodic oxidation method and PTh(polythiophene)/TiO_2 nanotube arrays electrode were obtained by electrochemical polymerization. X-ray powder diffraction (XRD) analysis confirmed the formation of TiO_2 phase. The morphologies and optical characteristics of the TiO_2 nanotube arrays were studied by scanning electron microscope (SEM), UV-Vis absorption spectra and Raman spectra. The results demonstrate that the PTh/TiO_2 electrode could enlarge the visible light absorption region and increase the photocurrent in visible region. The modified TiO_2 electrode with light-to-electric energy conversion efficiency of 1·46%, the short-circuit current density of 4·52 mAcm^{-2}, open-circuit voltage of 0·74 V and fill factor of 0·44, were obtained.**

Keywords. **TiO_2 nanotube arrays; anodization; polythiophene.**

1. Introduction

Since the dye-sensitized solar cell was reported in 1991 by O'Regan and Gratzel, solar energy conversion based on organic semiconductors became an emerging research field. It has been considered to hold new substantial future prospects and has attracted much attention for its many advantages such as easy fabrication, good flexibility and low cost (O'Regan and Grätzel 1991; Grätzel 2004; Kim *et al* 2006; Kuo *et al* 2008). Nowadays, the semiconductors with one-dimensional pattern, such as TiO_2 nanotubes, nanoparticles have gained significant attention as promising materials used in solar cells, photocatalysts, gas sensors and drug delivery for their peculiar chemical and physical properties (Varghere *et al* 2003; Ohsaki *et al* 2005; Mor *et al* 2005; Popat *et al* 2007). Many synthesis methods for fabricating TiO_2 nanotube arrays have been reported including anodic oxidation, sol–gel and electrophoresis deposition (Miao *et al* 2002; Lin *et al* 2003; Vega *et al* 2008; Liang and Li 2009; Mura *et al* 2009). Unfortunately, the bandgap of TiO_2 (3·0–3·2 eV) is too wide to absorb the visible light efficiently and it becomes photochemically active only under UV light irradiation, which results in limited practical applications. In order to extend the visible light response of TiO_2, many efforts have been made on bandgap engineering of titania such as element doping, organic dyes photosensitization, and coupling with a narrow bandgap semiconductor sensitization (Hsu *et al* 2005; Paulose *et al* 2006; Vitiello *et al* 2006). Titania nanotubes can be utilized to improve electron transport, provide larger surface area. Dye-sensitized solar cells with light-to-electric energy conversion efficiency of 5·42% has been achieved by incorporating 30% TiO_2 nanotube arrays into photoanode (Wang *et al* 2009). Although the results obtained are very impressive, there are still room for further improvement in the efficiency and stability through engineering new materials.

The advantages of using conjugated polymers as sensitizers are that they are relatively inexpensive compared to the more commonly used ruthenium based dyes and they have much higher absorption coefficiency (Coakley and McGehee 2004). PTh is photochemically and thermally stable under photoirradiation. And this conjugated polymer has a bandgap between the lowest unoccupied molecular orbital (LUMO) and the highest occupied molecular orbital (HOMO) of 2·02 eV, and a high absorption coefficient. These properties make it well suited for absorbing visible light in photovoltaic devices. Furthermore, when this polymer harvests visible light, an absorbed photon promotes an electron from the ground state of the polymer located in the semiconductor energy gap into an excited state that is in resonance with the CB. The polymer *p*-orbital becomes HOMO in the combined system. Since the lowest unoccupied molecular orbital LUMO levels of polymer are energetically higher than the conduction band edge of TiO_2, which is conducive to transfer electrons from the polymer to the nanotubes, thereby

*Author for correspondence (pqigx@163.com)

favoured the separation of electron and hole pairs and thus the photoelectric conversion efficiency could be improved.

Based on the above mentioned factors, in this study, we chose polythiophene as photosensitizer to be attached on the anodic TiO_2 nanotube arrays through a simple electropolymerization technique and thereby investigated the photoelectrochemical properties of polythiophene–TiO_2 nanotube arrays composites. Our samples consist of a vertically oriented TiO_2 nanotube array film on Ti foil substrate, whose geometrically ordered architecture has been demonstrated to result in enhanced light absorption and superior charge collection efficiencies in dye sensitized solar cells (Ong *et al* 2007; Zhu *et al* 2007; Wang *et al* 2009). Here, anodic oxidation of titanium foil in fluoride-based solutions was explored to synthesize TiO_2 nanotube arrays, which also offers a simplification of the whole process.

2. Experimental

2.1 *Preparation of TiO_2 nanotube arrays*

TiO_2 nanotube arrays were prepared by the anodic oxidation method. Small sheets of commercially available pure titanium were used as initiating materials. The samples had dimensions of 15 × 20 mm with a thickness of 0·5 mm. After ultrasonic cleaning by acetone, isopropanol, ethanol and deionized water, the titanium sheets were dried with nitrogen gas. Then the titanium sheet was set in a two-electrode cell containing an ethylene glycol solution with 0·25 wt% NH_4F and subjected to an anode voltage of 45 V generated by a potentiostat for 10 h. The counter electrode was a graphite stick. After anodization, all samples were washed in deionized water and dried with nitrogen gas. In order to transform amorphous TiO_2 nanotubes to the anatase phase, all samples were placed in a programmed temperature furnace for 3 h, the temperature was set at 450°C with a slope of 1°C/min in air.

2.2 *Characterization of TiO_2 nanotube arrays*

Powder X-ray diffraction (XRD, 40 kV and 30 mA, Cu Kα = 1·5406 Å Rigaku/Dmax-2500X, Japan) was used to identify the crystal phase of the final products. Scanning electron microscopy (SEM) of HITACHI S-3400N type was used to observe morphology of the samples. Raman spectra were recorded on a LabRAM Aramis Raman spectrophotometer. The UV-Vis absorption spectrum was recorded on a UV-2501PC spectrophotometer (Shimadzu, Japan). All measurements of phosphors were carried out at room temperature.

2.3 *Preparation of polythiophene modified TiO_2 nanotube arrays electrode*

A conventional three-electrode configuration with a platinum gauze as counter electrode and an Ag/AgCl as a reference electrode were used. The titanium sheets were set in a three-electrode cell containing a mixture solution of acetonitrile solution with 0·1 molL^{-1} thiophene monomer and diethyl ether solution with 0·01 molL^{-1} boron trifluoride and subjected to an anode voltage of 1·2 V generated by a potentiostat for 60 s.

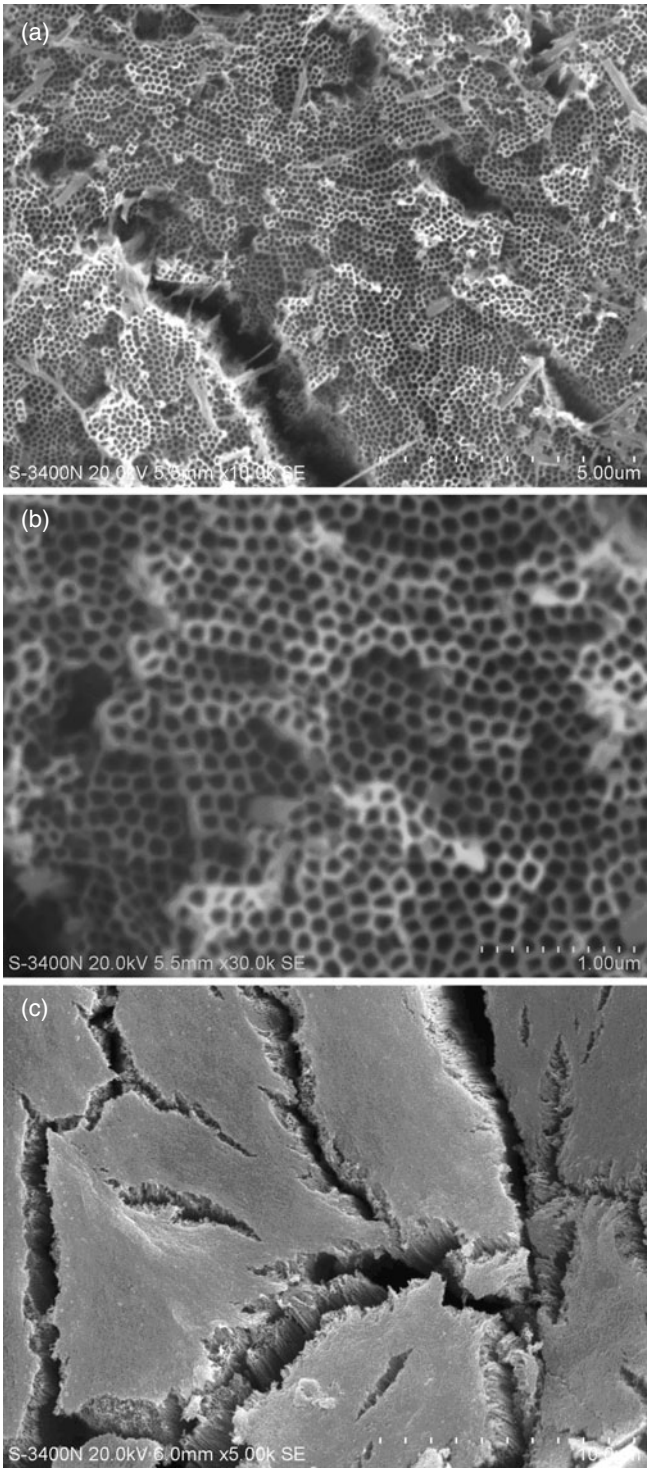

Figure 1. SEM images of (**a**, **b**) TiO_2 nanotube arrays and (**c**) polythiophene modified TiO_2 nanotube arrays.

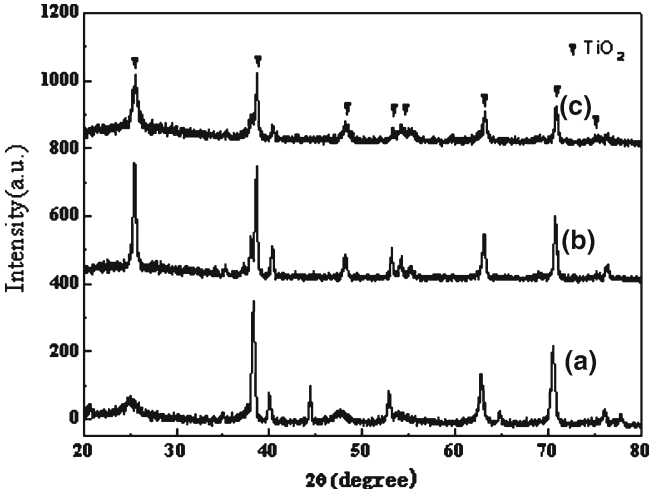

Figure 2. XRD patterns of (a) as-anodized TiO_2 nanotube arrays, (b) annealed TiO_2 nanotube arrays on Ti foil at 450°C and (c) polythiophene modified TiO_2 nanotube arrays, respectively.

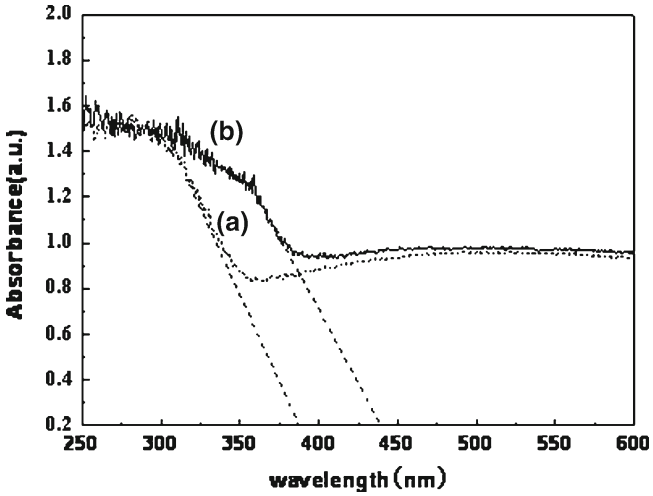

Figure 4. UV-Vis absorption spectra of (a) TiO_2 nanotube array films and (b) TiO_2/PTh nanotube array films.

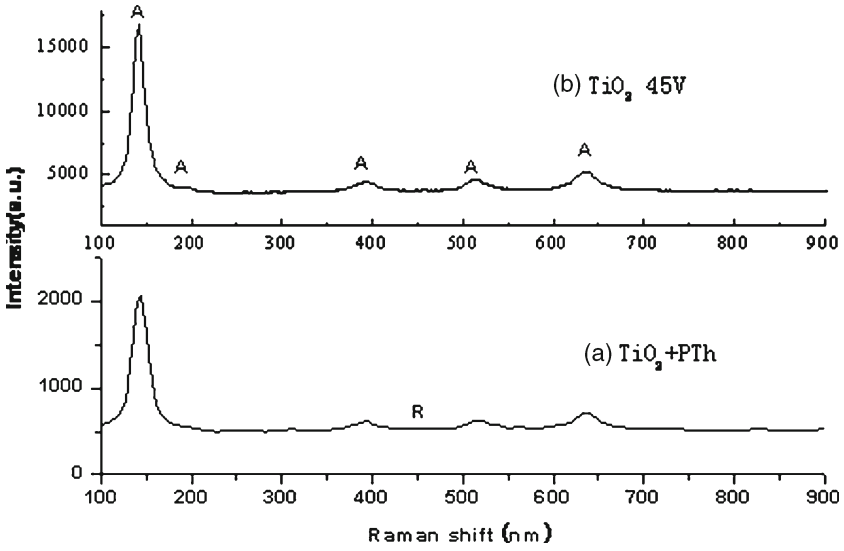

Figure 3. Raman spectra of (a) TiO_2/PTh nanotube array films and (b) TiO_2 nanotube array film.

2.4 *Characterization of photoelectric properties*

The photovoltaic test of polythiophene sensitized TiO_2 nanotube arrays electrode was carried out by measuring the *I–V* curves with conventional three-electrode system comprising of an Ag/AgCl reference electrode and Pt thread counter electrode using an Electrochemical Workstation (Model LK98BII). A 0·5 M Na_2S, 0·125 M S and 0·2 M KCl aqueous solution was used as the electrolyte. The working electrodes were irradiated under AM 1·5 simulated sunlight (100 mW/cm^2) with filtered light from a 500W Xenon arc lamp. All measurements were carried out under ambient conditions.

3. Results and discussion

3.1 *Morphology of TiO_2 nanotube arrays*

Figure 1(a, b) shows SEM images of TiO_2 nanotube arrays obtained by anodic oxidation method in ethylene glycol solution with 0·25 wt% NH_4F. Highly ordered TiO_2 nanotube arrays could be successfully fabricated by the anodization process and the inner diameter of nanotubes is about 100 nm as shown in figure 1(a). Figure 1(b) shows the magnified image of TiO_2 nanotube arrays of figure 1(a). It is apparent in figure 1(c) that the polythiophene modified TiO_2 nanotube arrays still keep nanotubular structure with no significant

morphology change, and nanotube arrays were covered with a layer of polymer surface.

3.2 *Crystalline formation of TiO_2 nanotube arrays*

Figure 2 (a, b and c) shows X-ray diffraction patterns of as-anodized TiO_2 nanotube arrays, annealed TiO_2 nanotube arrays on Ti foil at 450°C and polythiophene modified TiO_2 nanotube arrays, respectively. It can be seen from figure 2(a) that only the diffraction peaks of Ti appeared because the as-anodized TiO_2 nanotube arrays have an amorphous structure. However, after annealing process at 450°C for 3 h, the peaks of anatase crystalline structure of TiO_2 are shown in figure 2(b), which suggests that an amorphous phase of TiO_2 were crystallized into anatase phase by annealing at 450°C. The powder X-ray diffraction patterns of this sample show the TiO_2 phase to be consistent with Joint Committee on Powder Diffraction Standards (JCPDS) card No. 04-0477. The XRD patterns for polythiophene modified TiO_2 nanotube arrays are presented in figure 2(c), and it can be seen that the crystallized structures for modified samples still consist of anatase phase. After polymer modification, the intensity of XRD peaks decreased significantly, the intensity of XRD peaks reduced due to the TiO_2 surface which is covered by the polymer.

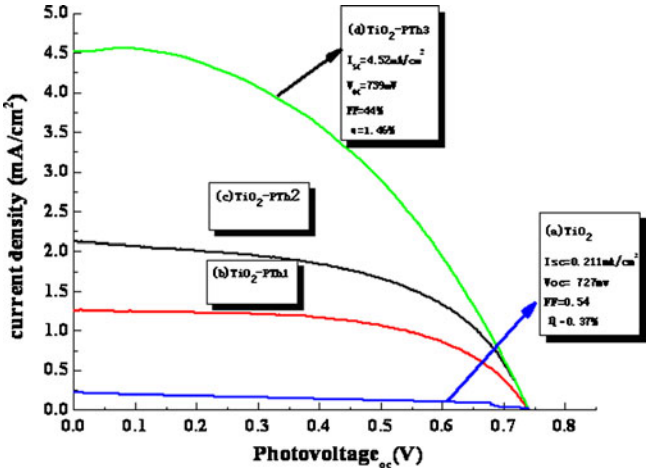

Figure 5. Photocurrent density generation of (a) TiO_2 nanotube arrays and (b) modified TiO_2 nanotube arrays under simulated sunlight irradiation (100 $mWcm^{-2}$).

3.3 *Raman spectra*

The crystalline formation of the TiO_2 nanotube arrays was also confirmed by Raman scattering (figure 3). TiO_2 exhibited six or four transition spectra for the anatase and rutile phases, respectively (Choi *et al* 2005). The Raman active mode of anatase phases is A_{1g} (519 cm^{-1}), B_{1g} (399 and 519 cm^{-1}) and E_g (144, 197, and 639 cm^{-1}). The Raman active mode of rutile phase is A_{1g}(612 cm^{-1}), B_{1g} (143 cm^{-1}), B_{2g} (826 cm^{-1}) and E_g(447 cm^{-1}). The amorphous TiO_2 showed a broad spectrum, while the annealed TiO_2 exhibited specific peaks at 144, 194, 391, 512 and 633 cm^{-1}, which are the signatures of the anatase TiO_2 (Wang *et al* 2008). After modification by the polymer, the intensity of specific peaks decreased, which resulted from the polymer suppressing the production of anatase.

3.4 *UV–vis absorption spectra*

The effects of polythiophene modifying on the light absorption characteristics of TiO_2 nanotube arrays are shown in figure 4. It can be seen from figure 4(a) that the bandgap energies of unmodified TiO_2 nanotube arrays is about 3·20 eV. Compared with the spectrum of unmodified TiO_2 nanotube arrays, the modified TiO_2 nanotube arrays exhibit stronger absorption in the UV–vis range (figure 4(b)). The modified sample exhibits red shifts in the bandgap transition due to the low bandgap of polythiophene (2·02 eV), and the absorption edge in the spectrum of modified TiO_2 nanotube arrays is about 2·80 eV, which would favour absorption of the solar energy in visible region. The results of the absorption feature suggest that the polythiophene modified TiO_2 nanotube arrays could be activated by visible light and it also could exhibit enhanced photoresponse under UV light.

3.5 *Photoelectrochemical properties*

The photocurrent densities based on TiO_2 nanotube array and polythiophene modified TiO_2 nanotube array as electrodes are shown in figure 5(a–d) and table 1. Clearly, the photocurrent densities of polythiophene modified samples are higher than that of unmodified one, which imply that more photoexcited electrons on the polythiophene modified TiO_2 electrode transport to the cathode, leaving more photoexcited holes involved in the oxidation reaction with the same bias potential. It is obvious that the voltage of the polythiophene modified TiO_2 electrode is higher

Table 1. Current–voltage characteristics of PTh–TiO_2 electrode fabricated at different lengths of TiO_2 nanotube arrays.

Nanotube length (μm)		J_{sc} ($mAcm^{-2}$)	V_{oc} (mV)	FF	E_{ff}%
(a) ∼5·0	Without-PTh	0·21	727	0·54	0·37
(b) ∼1·9	With-PTh1	1·26	760	0·56	0·57
(c) ∼3·2	With-Pth2	2·13	752	0·49	0·86
(d) ∼5·0	With-PTh3	5·48	740	0·44	1·46

than that of unmodified one. And with increase in the length of TiO_2 nanotube arrays, current density and photoelectric conversion efficiency of the cells were enhanced. As a result, a modified TiO_2 (length of about 5·0 μm) electrode with light-to-electric energy conversion efficiency of 1·46%, the short-circuit current density of 4·52 $mAcm^{-2}$, open-circuit voltage of 0·74 V and fill factor of 0·44 was obtained. Polymeric sensitizers are attractive because of the low cost and relatively large extinction coefficients compared to molecular dyes, which enable significant light harvesting using a much smaller photoelectrode thickness.

4. Conclusions

The highly ordered and uniform TiO_2 nanotube arrays were fabricated by anodic oxidation method, and the PTh/TiO_2 nanotube arrays electrode was obtained by electrochemistry polymerization method. Compared with the unmodified TiO_2 nanotube arrays, the modified TiO_2 nanotube arrays exhibit stronger absorption in the UV–vis range and the absorption border was moved from 3·20 eV to 2·80 eV, which would favour the absorption of the solar energy in visible region. A modified TiO_2 electrode with light-to-electric energy conversion efficiency of 1·46%, the short-circuit current density of 4·52 $mAcm^{-2}$, open-circuit voltage of 0·74 V and fill factor of 0·44 was achieved.

Acknowledgements

This research was supported by the National Science Foundation of China (Grant No. 20863008); the Natural Science Foundation of Guangxi Province (No. 0640206); the Open Foundation of Key Laboratory of Semiconductor Materials Science Institute of Semiconductors (KLSMS-0905).

References

Choi H C, Jung Y M and Kim S B 2005 *Vib. Spectrosc.* **37** 33
Coakley K M and McGehee M D 2004 *Chem. Mater.* **16** 4533
Grätzel M 2004 *J. Photochem. Photobiol. A Chem.* **164** 3
Hsu M C, Leu I C, Sun Y M and Hon M H 2005 *J. Cryst. Growth* **285** 642
Kim J Y, Kim S H, Lee H H, Lee K, Ma W, Gong X and Heeger A J 2006 *Adv. Mater.* **18** 572
Kuo C Y, Tang W C, Gau C, Guo T F and Jeng D Z 2008 *Appl. Phys. Lett.* **93** 0333071
Liang H C and Li X Z 2009 *J. Hazard Mater.* **162** 1415
Lin Y, Wu G S, Yuan X Y, Xie T and Zhang L D 2003 *J. Phys. Condens. Matter* **15** 2917
Miao Z, Xu D S, Ouyang J, Guo G, Zhao X and Tang Y 2002 *Nano Lett.* **2** 717
Mor G K, Shankar K, Paulose M, Varghese O K and Grimes C A 2005 *Nano Lett.* **5** 191
Mura F, Masci A, Pasquali M and Pozio A 2009 *Electrochim. Acta* **54** 3794
Ohsaki Y, Masaki N, Kitamura T, Wada Y, Okamoto T, Sekino T, Niihara K and Yanagida S 2005 *Phys. Chem. Chem. Phys.* **7** 4157
Ong K G, Varghese O K, Mor G K, Shankar K and Grimes C A 2007 *Sol. Energy Mater. Sol. Cells* **91** 250
O'Regan B and Grätzel M 1991 *Nature* **353** 737
Paulose M, Shankar K, Varghese O K, Mor G K and Grimes C A 2006 *J. Phys. D: Appl. Phys.* **39** 2498
Popat K C, Eltgroth M, LaTempa T J, Grimes C A and Desai T A 2007 *Small* **3** 1878
Varghere O K, Gong D, Paulose M, Ong K G and Grimes C A 2003 *Sensor Actuator* **B93** 338
Vega V *et al* 2008 *J. Non-Cryst. Solids* **354** 5233
Vitiello R P, Macak J M, Ghicov A, Tsuchiya H, Dick L F P and Schmuki P 2006 *Electrochem. Commun.* **8** 544
Wang D, Yu B, Zhou F, Wang C and Liu W 2009 *Chem. Phys.* **113** 602
Wang J and Lin Z Q 2008 *Chem. Mater.* **20** 1257
Zhu K, Neale N R, Miedaner A and Frank A J 2007 *Nano Lett.* **7** 69